Journal of Crystal Growth 311 (2009) 1559–1564

Contents lists available at ScienceDirect

Journal of Crystal Growth

journal homepage: www.elsevier.com/locate/jcrysgro

Polyol-mediated synthesis of well-dispersed α-$NaYF_4$ nanocubes

Ruifei Qin [a,c], Hongwei Song [b,*], Guohui Pan [a,c], Haifeng Zhao [a], Xinguang Ren [a], Lina Liu [a,c], Xue Bai [b], Qilin Dai [a,c], Xuesong Qu [a,c]

[a] Key Laboratory of Excited State Physics, Changchun Institute of Optics, Fine Mechanics and Physics, Chinese Academy of Sciences, 16 Eastern South-Lake Road, Changchun 130033, People's Republic of China

[b] State Key Laboratory of Integrated Optoelectronics, College of Electronic Sciences and Engineering, Jilin University, 2699 Qianjin Street, Changchun 130012, People's Republic of China

[c] Graduate School of Chinese Academy of Sciences, Beijing 100039, People's Republic of China

ARTICLE INFO

Article history:
Received 23 June 2008
Received in revised form
10 October 2008
Accepted 23 October 2008
Communicated by J.M. Redwing
Available online 17 November 2008

PACS:
61.46.+w
81.07.Bc
81.10.Dn

Keywords:
A1. Nanostructures
B1. Nanomaterials
B1. Rare earth compounds
B2. Phosphors

ABSTRACT

In this paper, well-dispersed α-$NaYF_4$ nanocubes were synthesized with a polyol method. The influence of molar ratio of $F^-/Y^{3+}/Na^+$ and type of polyol on the phase and morphology of the as-prepared $NaYF_4$ samples was examined. Formation process of these α-$NaYF_4$ nanocubes was traced via time-dependent experiments. Photoluminescence measurements demonstrated the as-prepared nanocubes are good up- and down-conversion luminescent host materials.

1. Introduction

Morphology- and size-controlled synthesis of various inorganic nanocrystals is vital to both the "bottom-up" self-assembly approach toward future nanodevices and the investigation of their morphology- and size-dependent properties. $NaYF_4$ has drawn more attention because hexagonal $NaYF_4$ (β-$NaYF_4$) is the most efficient host material for green and blue up-conversion phosphors up to now. Lanthanide-doped $NaYF_4$ nanocrystals have potential uses in high-resolution displays, integrated optical systems, solid-state lasers and especially biological labels, so both cubic (α-phase) and hexagonal (β-phase) $NaYF_4$ nanocrystals with various sizes and morphologies have been synthesized via various methods [1–28]. Using EDTA, citrate and oleate as chelating agents, α-$NaYF_4$ nanoparticles can be prepared with wet chemical approaches [1–9]. α-$NaYF_4$ nanoparticles can also be prepared with a polyol method and modified coprecipitation method [10–13]. β-$NaYF_4$ nanoparticles have been fabricated solvothermally in the presence of EDTA and applied to the sensitive detection of trace amounts of targeted biomolecules [14–17]. Li et al. [6,7,18] have developed a facile solution route for preparing uniform single-crystal β-$NaYF_4$ nanorods and hexagonal nanoplates. Very recently, α-$NaYF_4$ nanoparticles and β-$NaYF_4$ nanoparticles, nanorods and hexagonal nanoplates have been synthesized by cothermolysis of yttrium trifluoroacetate ($Y(CF_3COO)_3$) and sodium trifluoroacetate ($NaCF_3COO$) in high-temperature organic solutions [19–26].

The morphology of a crystal is determined by its crystal structure and growth surroundings. For example, hexagonal crystal seeds have an anisotropic unit cell structure, which can induce anisotropic growth along crystallographically reactive directions, and thus hexagonal shaped nanoplates or nanorods were usually obtained; for a crystal with a cubic crystal structure, a cubic or spherical shape is expected depending on growth surroundings. For α-$NaYF_4$, to the best of our knowledge, spherical shape was often obtained, however cubic shape was seldom obtained. α-$NaYF_4$ nanocubes of ~10–13 nm in diameter have been obtained solvothermally in water/alcohol/oleic acid systems [6,7]. Truncated α-$NaYF_4$ nanocubes of 5.1 ± 0.6 nm were synthesized from trifluoroacetate precursors in a hot surfactant solution

*Corresponding author. Fax: 86 431 86176320.
E-mail address: hwsong2005@yahoo.com.cn (H. Song).

0022-0248/$ - see front matter © 2008 Elsevier B.V. All rights reserved.
doi:10.1016/j.jcrysgro.2008.10.113

[20]. Being covered with oleic acids, these α-$NaYF_4$ nanocubes can only be transparently dispersed in nonpolar solvent. For some applications, for example, biological labels, nanocrystals should be able to be dispersed in aqueous solution, so surface modification of the nanocubes is needed to render their water solubility. In this paper, we synthesized α-$NaYF_4$ nanocubes with a polyol method. These α-$NaYF_4$ nanocubes could be well-dispersed in water to form a colloidal solution. The influence of molar ratio of $F^-/Y^{3+}/Na^+$ and type of polyol on the phase and morphology of the as-prepared $NaYF_4$ samples was examined. Photoluminescence measurements demonstrated the as-prepared α-$NaYF_4$ nanocubes are good luminescent host materials.

2. Experimental section

2.1. Preparation

All chemicals were of analytical grade and were used as received. Deionized water was used throughout. In a typical synthesis of $NaYF_4$ nanocubes, 10 mmol NH_4F was dissolved in 20 mL ethylene glycol (EG). Afterwards a solution of 2 mmol $Y(NO_3)_3 \cdot 6H_2O$ and 2 mmol $NaNO_3$ in 20 mL EG was added under vigorous stirring. The molar ratio of $F^-/Y^{3+}/Na^+$ was 5:1:1. After stirring for 30 min, the mixed solution was transferred into a Teflon bottle of 50 mL held in a stainless steel autoclave, sealed, and maintained at 180 °C for 24 h. After cooling to room temperature, the product was collected by centrifugation and washed several times with water and ethanol and finally dried at 80 °C for 12 h in vacuum.

2.2. Characterization

X-ray diffraction (XRD) patterns were recorded on a Rigaku D/max-rA diffractometer with CuKα-radiation resource (λ=1.54078 Å). The morphologies of products were observed using a field emission scanning electron microscope (FE-SEM, Hitachi S-4800) and a transmission electron microscope (TEM, JEM 2010) operated at 200 kV. The photoluminescence spectra were recorded with a Hitachi F-4500 spectrophotometer equipped with a 150 W xenon lamp source. The up-conversion fluorescence spectrum was obtained on the Hitachi F-4500 fluorescence spectrophotometer under the excitation of a 980-nm laser diode.

3. Results and discussion

3.1. Structure and morphology

The XRD pattern of the typical sample and the standard data of α-$NaYF_4$ (JCPDS, Card no. 77-2042) are depicted in Fig. 1a. The XRD pattern agrees well with the standard data. So the typical sample is α-$NaYF_4$. The broadening of the diffraction peaks reveals the nanocrystalline nature of the sample. An EDAX result confirms the main elemental components are Na, Y and F (Fig. 1b).

Fig. 1c shows a FE-SEM image of the typical sample. It can be seen that the sample is composed of well-dispersed nanocubes with a mean edge length of about 30 nm. The surface of these nanocubes is smooth, and the size distribution of them is broad to some degree. A TEM image of the typical sample shown in Fig. 1d is consistent with the FE-SEM image. It should be noted that the majority of these nanocubes are well-defined and the others may not grow entirely.

3.2. Effect of molar ratio of $F^-/Y^{3+}/Na^+$

We found that the molar ratio of $F^-/Y^{3+}/Na^+$ (R) could effect not only the crystal structure but also the size and morphology of the product under our experimental conditions. Fig. 2a depicts XRD patterns of the products synthesized with different amounts of NH_4F keeping other conditions same as those for the typical synthesis. As can be seen from Fig. 2a, when R is 4:1:1, namely stoichiometric, the XRD pattern is α-$NaYF_4$ phase and no other phases can be identified by XRD. When the amount of NH_4F is increased until R reaches 7:1:1, the XRD pattern has no obvious changes. When R is 8:1:1, a small amount of β-$NaYF_4$

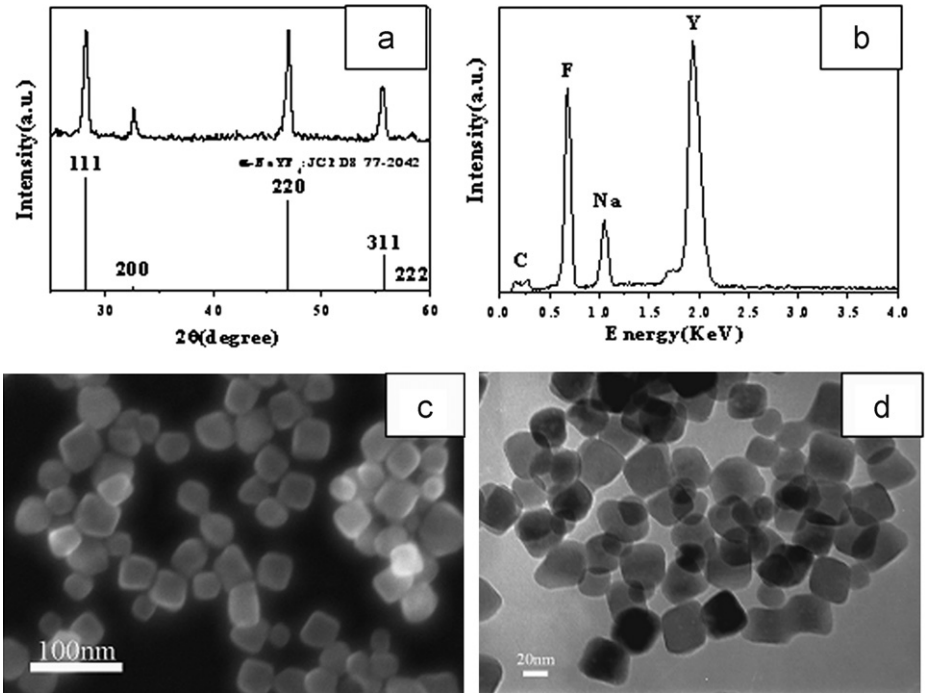

Fig. 1. (a) The standard data of α-$NaYF_4$ (JCPDS 77-2042) as a reference and XRD pattern, (b) EDAX spectrum, (c) FE-SEM image and (d) TEM image of the typical sample.

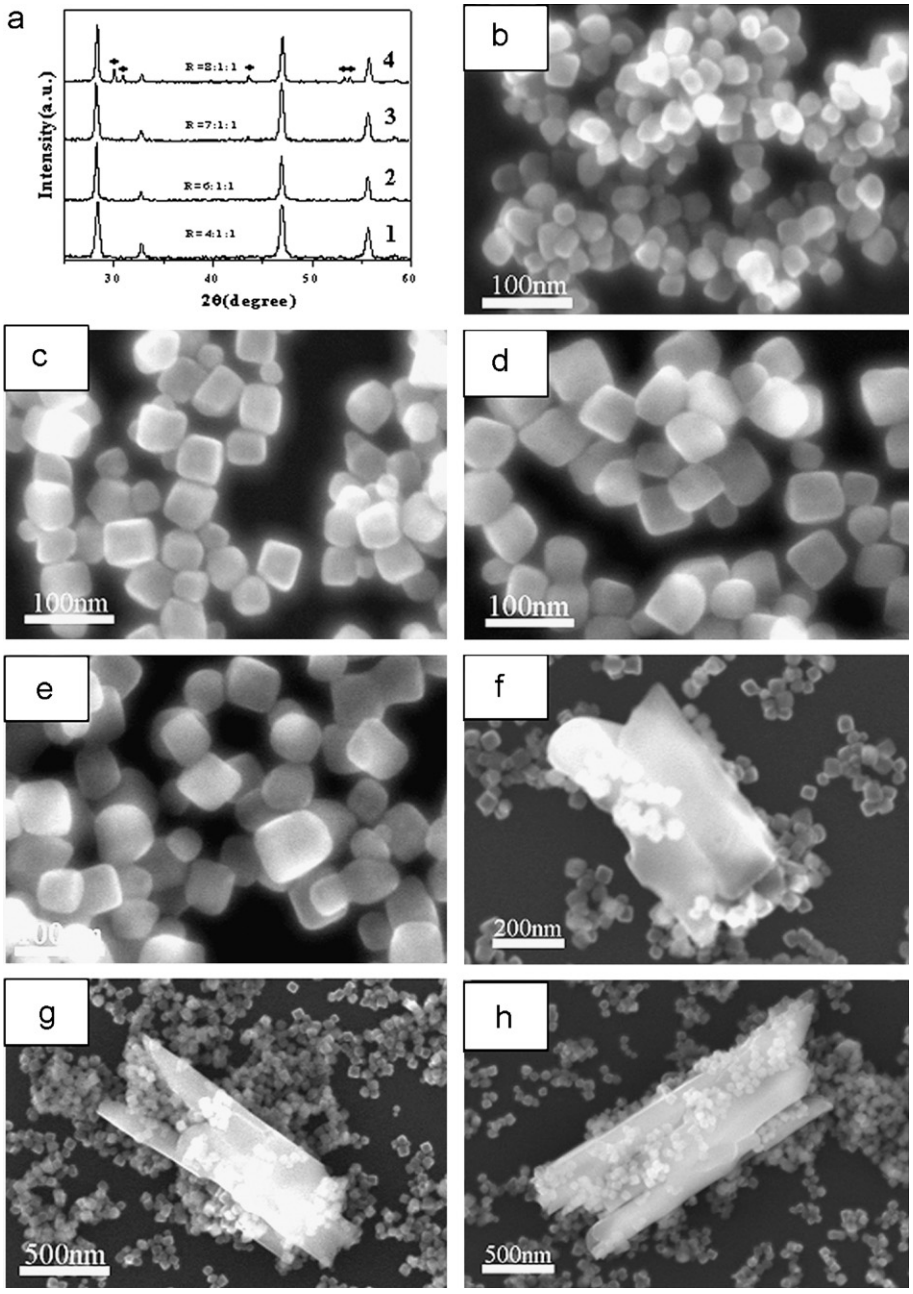

Fig. 2. (a) XRD patterns of $NaYF_4$ samples derived at different R values: (1) R=4:1:1, (2) R=6:1:1, (3) R=7:1:1, (4) R=8:1:1. FE-SEM images of $NaYF_4$ samples derived at different R values: (b) R=4:1:1, (c) and (f) R=6:1:1, (d) and (g) R=7:1:1, (e) and (h) R=8:1:1.

(marked with asterisks) emerges in the XRD pattern. Therefore under these experimental conditions, when the amount of NH_4F is large enough, a small amount of β-$NaYF_4$ will exist in the product. We think NH_4F acts as both a reactant and a mineralizer and the presence of excess NH_4F favors the transform from α-$NaYF_4$ to β-$NaYF_4$ [2].

For bulk $NaYF_4$, cubic phase is the metastable high-temperature phase, while hexagonal phase is the thermodynamically stable low-temperature phase [19,28,29]. However, α-$NaYF_4$ tends to be formed first and then transforms to β-$NaYF_4$ under thermal treatment in most cases for solution-phase synthesis of $NaYF_4$. Under our experimental conditions, when the amount of NH_4F is large enough, a small amount of α-$NaYF_4$ will transform to β-$NaYF_4$. α-$NaYF_4$ generally transforms to β-$NaYF_4$ completely when a hydrothermal method is used. EG which acts as not only a solvent but also a capping ligand in our synthesis system can suppress the cubic-to-hexagonal phase transition and results in the incomplete transform from cubic phase to hexagonal phase [11]. Figs. 2b–h show FE-SEM images of the products corresponding to different R values. As can be seen from Figs. 2b–e and Fig. 1c, the morphology of the nanocubes becomes more and more regular and the mean edge length of the nanocubes becomes bigger and bigger with increasing amount of NH_4F. For the R value of 4:1:1, the morphology of the nanocubes is irregular. The mean edge lengths of the nanocubes are about 25, 30, 40, 50 and 50 nm for the R values 4:1:1, 5:1:1, 6:1:1, 7:1:1 and 8:1:1, respectively. It shoud be pointed out that there exist a very small number of submicrorods besides the dominating nanocubes in the products corresponding to the R values 6:1:1, 7:1:1 and 8:1:1, and that the number and size of the sub-microrods both increase with increasing amount of NH_4F (see Figs. 2f–h). We index these submicrorods to β-$NaYF_4$ and we think that β-$NaYF_4$ cannot be

detected by XRD due to its very small amount in the products corresponding to the R values 6:1:1 and 7:1:1.

The shape of an fcc nanocrystal is mainly determined by the ratio (R') between the growth rates along $\langle 1\,0\,0 \rangle$ and $\langle 1\,1\,1 \rangle$ directions. Octahedra and tetrahedra bounded by the most stable {1 1 1} planes will be formed when R'=1.73, and perfect cubes bounded by the less stable {1 0 0} planes will result if R' is reduced to 0.58 [30,31]. As illustrated above, the more NH_4F was used, the more regular the morphology of the nanocubes was. Excessive F^- inevitably capped on the crystal surface due to the strong coordination effect between F^- and Y^{3+} [7]. The different interactions between F^- and various crystallographic planes of fcc $NaYF_4$ may reduce the growth rate along the $\langle 1\,0\,0 \rangle$ direction and/or enhance the growth rate along the $\langle 1\,1\,1 \rangle$ direction, and thus may reduce R' to be close to 0.58. Thus excessive NH_4F is necessary for the formation of regular $NaYF_4$ nanocubes in our synthetic route.

3.3. Effect of reaction time-formation process

To study the formation process of these nanocubes, we carried out time-dependent experiments under the reaction conditions same as those for the typical synthesis except for the reaction time. Fig. 3a depicts XRD patterns of samples as a function of reaction time. The reaction time being 0 min means the sample is collected immediately after deposition at room temperature without any thermal treatment. It can be seen that all the samples are well-crystallized and can be assigned to the α-$NaYF_4$ phase, even if when the reaction time is 0 min, and that the crystallinity becomes better and better with prolonging reaction time.

Figs. 3b–f show FE-SEM images of $NaYF_4$ samples as a function of reaction time. When the reaction time is 0 min, the as-obtained $NaYF_4$ consists of quasi-spherical or cubic agglomerates with an average diameter of 65 nm (Fig. 3b). Individual agglomerate seems to be also composed of smaller nanoparticles with a size of several nanometers. These agglomerates seem to connect with one another. When the reaction time is 15 min, these agglomerates become more separate and smaller nanoparticles arrange more compact compared with the sample with a reaction time of 0 min (Fig. 3c). By prolonging the reaction time, these agglomerates evolve into quasi-cubic nanoparticles whose surface is coarse (see Fig. 3d). These quasi-cubic nanoparticles have a mean edge length of about 40 nm. When the reaction time is 80 min, the cubic morphology of the sample has been obvious and the surface of the nanocubes is smooth (Fig. 3e). With further prolonging the reaction time to 5 h, the cubic morphology becomes more regular and the surface of the nanocubes gets smoother compared with those of the sample with reaction time 80 min (Fig. 3f).

It is well known that the crystal structure and the growth surroundings of a material determine its final morphology. According to the time-dependent experiments, the formation process of these $NaYF_4$ nanocubes is as follows. The liquid precipitation reaction among $NaNO_3$, $Y(NO_3)_3$ and NH_4F in EG at

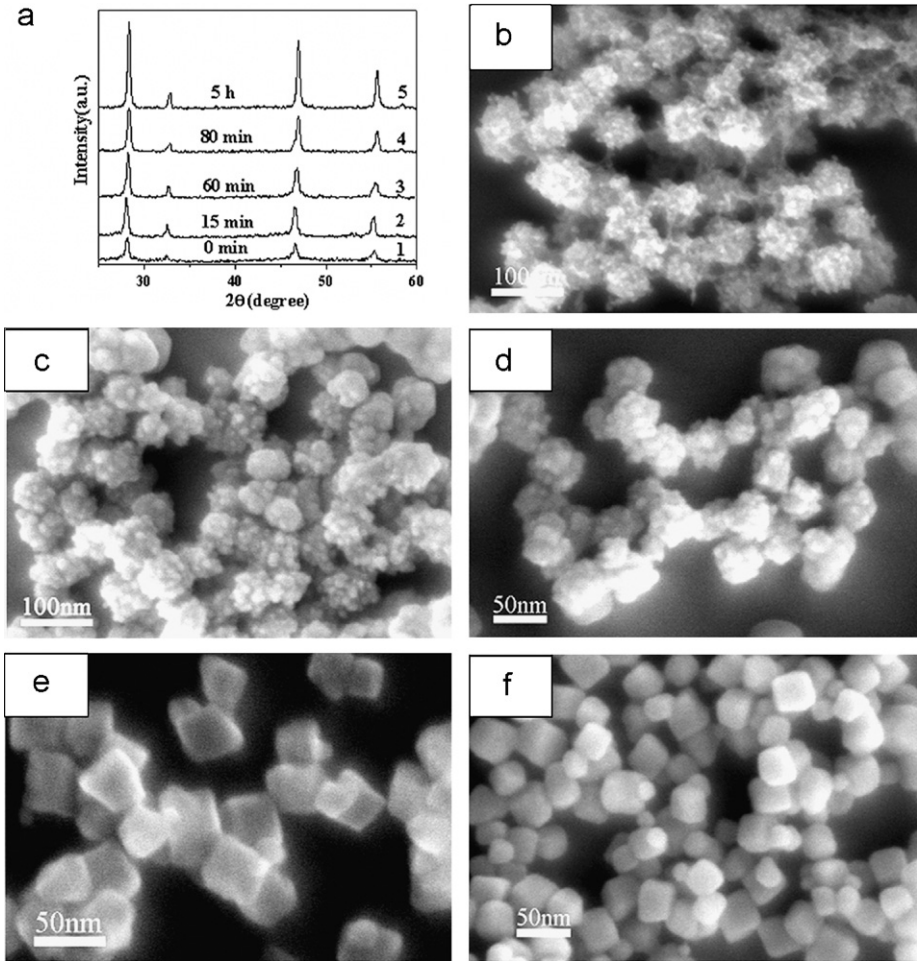

Fig. 3. (a) XRD patterns of $NaYF_4$ samples with different reaction times: (1) 0 min, (2) 15 min, (3) 60 min, (4) 80 min, (5) 5 h. FE-SEM images of $NaYF_4$ samples with different reaction times: (b) 0 min, (c) 15 min, (d) 60 min, (e) 80 min, (f) 5 h.

room temperature yields $NaYF_4$ agglomerates of diameter ~65 nm and composed of smaller nanoparticles. This morphology of $NaYF_4$ presumably stabilizes the possible high-energy surfaces of the smaller nanoparticles. Then these $NaYF_4$ agglomerates gradually evolve into $NaYF_4$ nanocubes by surface reconstruction due to the cubic crystal structure of $NaYF_4$. Presumably, this cubic morphology is thermodynamically more stable under the current synthetic conditions.

3.4. Effect of the type of polyol

The type of polyol was found to have an important effect on the morphology of the product. Diethylene glycol (DEG), glycerol (Glyc.) as well as Methanol (MeOH) were used to replace EG as the solvent to synthesize the samples discussed below. Fig. 4a shows XRD patterns of three samples synthesized using MeOH, DEG and Glyc. as solvents. For all three samples, the position of every diffraction peak is consistent with the standard data of α-$NaYF_4$ (JCPDS, Card no. 77-2042), indicating these samples crystallize in a cubic structure of $NaYF_4$, but the relative peak strength of ⟨220⟩ to ⟨111⟩ peak is stronger compared with the standard data, indicating the possibility of preferential orientation growth under these experimental conditions.

Panels b–d of Fig. 4 show FE-SEM images of the samples synthesized using MeOH, DEG and Glyc. as solvent, respectively. When MeOH and DEG were used, both the sampes are branched nanocrystals and are similar in shape, while when Glyc. was used, the majority of the nanocrystals in the sample have a cubic morphology with a mean edge length of about 30 nm. Liang et al. [27] have synthesized branched $NaYF_4$ nanocrystals by using CTAB as regulating agents in a MeOH/water system. They thought the adsorption effect of CTAB and MeOH on different crystal planes and the influence of micelles formed by CTAB were main factors influencing the formation of the branched structures. Branched gold nanocrystals have also been synthesized in aqueous solution at room temperature [32]. The different adsorption effects of molecules (CTAB and/or ascorbic acid) on different crystal planes were believed to result in the gold branched structure. In our experiments, MeOH and DEG may have a similar adsorption effect on different crystal planes and as a result branched $NaYF_4$ nanocrystals were obtained, while Glyc. and EG have another similar adsorption effect on different crystal planes and result in $NaYF_4$ nanocubes. On the basis of the above discussion, we can conclude that $NaYF_4$ nanocubes can only be obtained using certain polyols.

3.5. Photoluminescence of Yb^{3+}/Er^{3+} and Ce^{3+}/Tb^{3+} co-doped α-$NaYF_4$ nanocubes

To examine the feasibility of the as-prepared α-$NaYF_4$ nanocubes as efficient up-conversion and down-conversion host materials, Yb^{3+}/Er^{3+} and Ce^{3+}/Tb^{3+} ion pairs were, respectively, co-doped into the typical sample. As shown in Fig. 5a, these nanocubes can be well dispersed in water to form a colloidal solution. The up-conversion spectrum of a 1 wt% colloidal solution of α-$NaYF_4$: 4% Yb^{3+}, 1% Er^{3+} nanocubes in water under 980 nm laser diode excitation is shown in Fig. 5b. Emission peaks at 519, 538, and 650 nm are assigned, respectively, to transitions from $^4H_{11/2}$, $^4S_{3/2}$, and $^4F_{9/2}$ to $^4I_{15/2}$ of Er^{3+}. The inset of Fig. 5b shows a digital photograph of the up-conversion luminescence of the colloidal solution under the same excitation conditions. The luminescence appears yellow–green in color due to a combination of green and red emissions from the Er^{3+} ion.

Fig. 5c shows the excitation (left) and the emission (right) spectra of a 1 wt% colloidal solution of α-$NaYF_4$: 5% Ce^{3+}, 5% Tb^{3+} nanocubes in water. The spectra closely match what has been reported previously for the Ce^{3+}/Tb^{3+} ion pair in fluoride-based nanocrystals [33,34]. The broad excitation band from 200 to 300 nm is in good agreement with the 4f–5d absorption of Ce^{3+} ion. The emission spectrum is characteristic of the Tb^{3+} ion with the green band emission centered at 540 nm being dominant. The above results indicate the efficient energy transfer from Ce^{3+} to

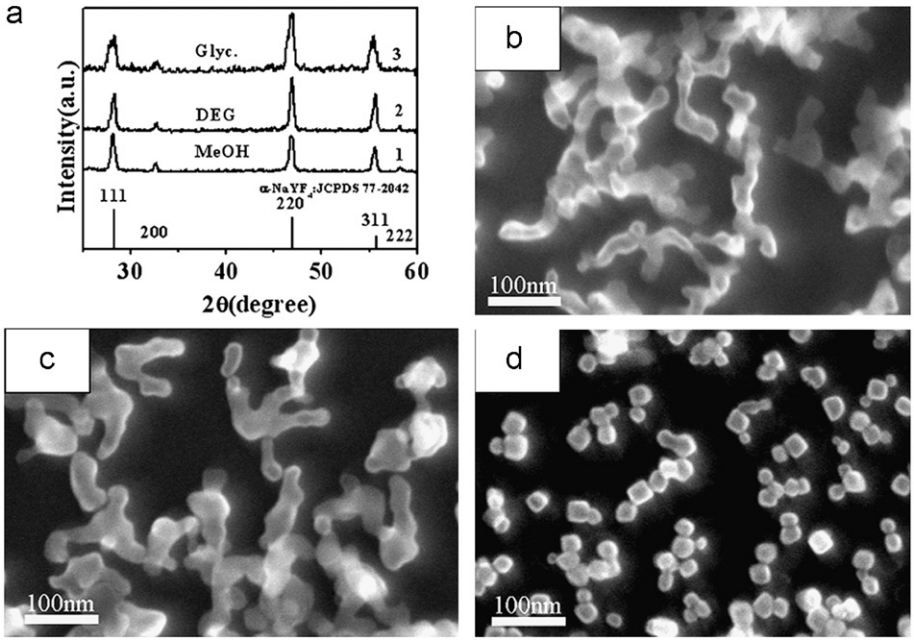

Fig. 4. (a) The standard data of α-$NaYF_4$ (JCPDS 77-2042) as a reference and XRD patterns of $NaYF_4$ samples with different polyols: (1) MeOH, (2) DEG, (3) Glyc. FE-SEM images of $NaYF_4$ samples with different polyols: (b) MeOH, (c) DEG, (d) Glyc..

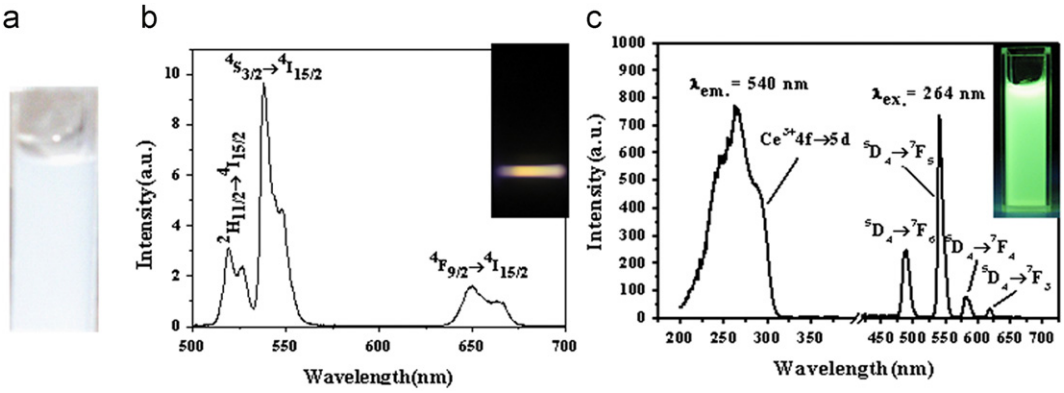

Fig. 5. (a) A photograph of the 1 wt% colloidal solution of $NaYF_4$ nanocubes in water. (b) The up-conversion spectrum of a 1 wt% colloidal solution of $NaYF_4$:4%Yb^{3+}, 1%Er^{3+} nanocubes in water under 980 nm laser diode excitation (laser power density $\approx$150 W/cm^2, EM slit=2.5 nm). Inset: a photograph of the up-conversion luminescence of the same solution under the same excitation conditions. (c) The excitation (left) and emission (right) spectra of a 1 wt% colloidal solution of $NaYF_4$:5%Ce^{3+}, 5%Tb^{3+} nanocubes in water (EX and EM slits=2.5 nm). Inset: a photograph of the same solution obtained under 254 nm ultraviolet light.

Tb^{3+}. The intense green emission of the colloidal solution is demonstrated in the inset of Fig. 5c with the digital photograph obtained under 254 nm ultraviolet light. These results demonstrate that the as-prepared α-$NaYF_4$ nanocubes are good luminescent host materials and that these co-doped samples have potentials as fluorescent labels.

4. Conclusions

In summary, well-dispersed α-$NaYF_4$ nanocubes have been synthesized with the simple polyol method. The molar ratio of $F^-/Y^{3+}/Na^+$ and the type of polyol both have effects on the phase and morphology of the as-prepared $NaYF_4$ samples. The morphology of the nanocubes becomes more and more regular and the mean edge length of the nanocubes becomes bigger and bigger with increasing amount of NH_4F. When the amount of NH_4F is larger, a small amount of α-$NaYF_4$ nanocubes will transform to β-$NaYF_4$ sub-microrods. Possibly due to different adsorption effects on different crystal planes, MeOH and DEG result in the formation of branched α-$NaYF_4$ nanocrystals, while Glyc. and EG result in α-$NaYF_4$ nanocubes. Time-dependent experiments reveal that as-prepared α-$NaYF_4$ nanocubes are formed by surface reconstruction of α-$NaYF_4$ agglomerates due to the cubic crystal structure. Photoluminescence measurements demonstrate the as-obtained nanocubes are good up- and down-conversion luminescent host materials.

Acknowledgement

This work was supported by High-Tech Research and Development Program of China (863) (Grant no. 2007AA03Z314), National Natural Science Foundation of China (Grant nos. 10374086, 10504030 and 10704073) and Talent Youth Foundation of Jilin Province (Grant no. 20040105).

References

[1] G.S. Yi, H.C. Lu, S.Y. Zhao, Y. Ge, W.J. Yang, D.P. Chen, L.H. Guo, Nano Lett. 4 (2004) 2191.
[2] Z.J. Wang, F. Tao, L.Z. Yao, W.L. Cai, X.G. Li, J. Crystal Growth 290 (2006) 296.
[3] Y.J. Sun, Y. Chen, L.J. Tian, Y. Yu, X.G. Kong, Nanotechnology 18 (2007) 275609.
[4] C.X. Li, J. Yang, Z.W. Quan, P.P. Yang, D.Y. Kong, J. Lin, Chem. Mater. 19 (2007) 4933.
[5] C.X. Li, Z.W. Quan, J. Yang, P.P. Yang, J. Lin, Inorg. Chem. 46 (2007) 6329.
[6] L.Y. Wang, Y.D. Li, Chem. Mater. 19 (2007) 727.
[7] X. Liang, X. Wang, J. Zhuang, Q. Peng, Y.D. Li, Adv. Funct. Mater. 17 (2007) 2757.
[8] X. Wang, J. Zhuang, Q. Peng, Y.D. Li, Nature 437 (2005) 121.
[9] X. Wang, J. Zhuang, Q. Peng, Y.D. Li, Inorg. Chem. 45 (2006) 6661.
[10] Z.Q. Li, Y. Zhang, Angew. Chem. Int. Ed. 45 (2006) 7732.
[11] Y. Wei, F.Q. Lu, X.R. Zhang, D.P. Chen, J. Alloys Compd. 455 (2008) 376.
[12] H. Schafer, K. Kompe, H.U. Gudel, M. Haase, Adv. Mater. 16 (2004) 2102.
[13] H. Schafer, P. Ptacek, K. Kompe, M. Haase, Chem. Mater. 19 (2007) 1396.
[14] J.H. Zeng, J. Su, Z.H. Li, R.X. Yan, Y.D. Li, Adv. Mater. 17 (2005) 2119.
[15] J.H. Zeng, Z.H. Li, J. Su, L.Y. Wang, R.X. Yan, Y.D. Li, Nanotechnology 17 (2006) 3549.
[16] L.Y. Wang, Y.D. Li, Chem. Commun. 24 (2006) 2557.
[17] L.Y. Wang, R.X. Yan, Z.Y. Hao, L. Wang, J.H. Zeng, J. Bao, X. Wang, Q. Peng, Y.D. Li, Angew. Chem. Int. Ed. 44 (2005) 6054.
[18] L.Y. Wang, Y.D. Li, Nano Lett. 6 (2006) 1645.
[19] H.X. Mai, Y.W. Zhang, R. Si, Z.G. Yan, L.D. Sun, L.P. You, C.H. Yan, J. Am. Chem. Soc. 128 (2006) 6426.
[20] H.X. Mai, Y.W. Zhang, L.D. Sun, C.H. Yan, J. Phys. Chem. C 111 (2007) 13730.
[21] J.C. Boyer, F. Vetrone, L.A. Cuccia, J.A. Capobianco, J. Am. Chem. Soc. 128 (2006) 7444.
[22] J.C. Boyer, L.A. Cuccia, J.A. Capobianco, Nano Lett. 7 (2007) 847.
[23] G.S. Yi, G.M. Chow, Adv. Funct. Mater. 16 (2006) 2324.
[24] G.S. Yi, G.M. Chow, Chem. Mater. 19 (2007) 341.
[25] J.N. Shan, Y.G. Ju, Appl. Phys. Lett. 91 (2007) 123103.
[26] J.N. Shan, X. Qin, N. Yao, Y.G. Ju, Nanotechnology 18 (2007) 445607.
[27] X. Liang, X. Wang, J. Zhuang, Q. Peng, Y.D. Li, Inorg. Chem. 46 (2007) 6050.
[28] Y. Wei, F.Q. Lu, X.R. Zhang, D.P. Chen, Chem. Mater. 18 (2006) 5733.
[29] R.E. Thoma, H. Insley, G.M. Hebert, Inorg. Chem. 5 (1966) 1222.
[30] Y.G. Sun, Y.N. Xia, Science 298 (2002) 2176.
[31] Z.L. Wang, J. Phys. Chem. B 104 (2000) 1153.
[32] S.H. Chen, Z.L. Wang, J. Ballato, S.H. Foulger, D.L. Carroll, J. Am. Chem. Soc. 125 (2003) 16186.
[33] J.C. Boyer, J. Gagnon, L.A. Cuccia, J.A. Capobianco, Chem. Mater. 19 (2007) 3358.
[34] L.Y. Wang, Y.D. Li, Chem. Eur. J. 13 (2007) 4203.